SciForum
Mol2Net

New Insights from the CoMSIA Analysis within the Framework of Density Functional Theory

Alejandro Morales-Bayuelo * and Julio Caballero
Centro de Bioinformática y Simulación Molecular (CBSM), Universidad de Talca, 2 Norte 685, Casilla 721, Talca, Chile
* Author to whom correspondence should be addressed; E-Mail: alejandr.morales@uandresbello.edu.

Published: 4 December 2015

Abstract: Today, one of the main aims in the pharmaceutical companies is seek new methodologies to understand the biological activity in molecules from the computational point of view. In this sense, understand the traditional tools (3D QSAR) such as the Comparative Molecular Similarity Analysis (CoMSIA) within the quantum chemistry framework, can be relevant. In this context, the quantification of steric and electrostatic effects on a serie of antimalarials chalcones was performed on the basis of the descriptors from the molecular quantum similarity field and chemical reactivity supported in DFT. The steric and electrostatic effects were studied using scales of convergence quantitative alpha (α) and beta (β), respectively. To deal the problem of relative molecular orientation in the quantum similarity field the Topo-Geometrical Superposition Algorithms (TGSA) was used as molecular alignment method. Finally, a chemical reactivity analysis using global and local descriptors such as chemical hardness, softness, electrophilicity, and Fukui Functions was developed.
.
.

Keywords: Antimalarials Chalcones, Comparative Molecular Similarity Indexes Analysis (CoMSIA), 3D-QSAR, Molecular Quantum Similarity (MQS), Chemical Reactivity Descriptors, Density Functional Theory (DFT)

1. Introduction

In a recent publication our researcher group shown as the Comparative Molecular Field Analysis (CoMFA) can be understood in terms of Molecular Quantum Similarity (MQS) and Density Functional Theory (DFT)-based reactivity descriptors **[1]**. The CoMFA analysis have many applications in the three-Dimensional Quantitative Structure-Activity Relationships (3D QSAR) studies, yet this method is commonly associated with the Comparative Molecular Similarity Indexes Analysis (CoMSIA) by this reason in this work is studied

the CoMSIA analysis in terms of MQS and chemical reactivity descriptors to search new insights within the DFT framework.

The MQS field was introduced by Carbó and co-workers approximately 35 years ago **[2-5]**, this is a topic which has been widely considered and applied on chemical phenomenon study such as electron delocalization and aromaticity **[6]**, modeling 3D QSAR **[7]**, topological studies **[8]**, among others. The MQS field the main variable is the density function **[9-11]**; of this form can be related with the chemical reactivity descriptors such as chemical hardness (η), softness (S), electrophilicity (ω) and Fukui Functions. Therefore, using this hybrid methodology (joining the MQS and chemical reactivity) we hope show how the CoMSIA results can be related with the DFT context.

To the carry out these goals, we used the CoMSIA results reported by Xue and co-workers **[12]**. They development a 3D QSAR studies on antimalarial alkoxylated and hydroxylated chalcones by CoMFA and CoMSIA to determine the factors required for the activity of these compounds, this study shown that the CoMSIA analysis presents better physical-chemistry parameters to understand the antimalarial activity using five physical-chemistry properties (steric, electrostatic, hydrophobic, and hydrogen-bond donor or acceptor properties). In line, with this reported we will use the hybrid methodology proposed to modeling and study these CoMSIA outcomes using DFT.

Furthermore, the entropic contributions to the binding affinity are more difficult to describe using the CoMSIA methodology, because a major factor arises from the solvent-to-protein transfer. This portion approximately correlates with the size of the hydrophobic surface area of the drug molecule **[13, 14]**. For these reasons, show new methodologies are relevant in the QSAR field.

2. Molecular Set

A series of chalcones studied by Xue and co-workers **[12]** were used in this study. The biological activity IC_{50} values μM (for inhibition of [3H] hypoxanthine uptake into *P. falciparum* (K1) in the presence of drug) were expressed as pIC_{50} (the –log IC_{50}), these biological values were reported by Liu and co-workers **[15]**, the theoretical values from the CoMSIA method are shown in **Table 1 [12]**.

Table 1. Compounds, biological activities and theoretical predictions from the CoMSIA method in the molecular set **[12]**.

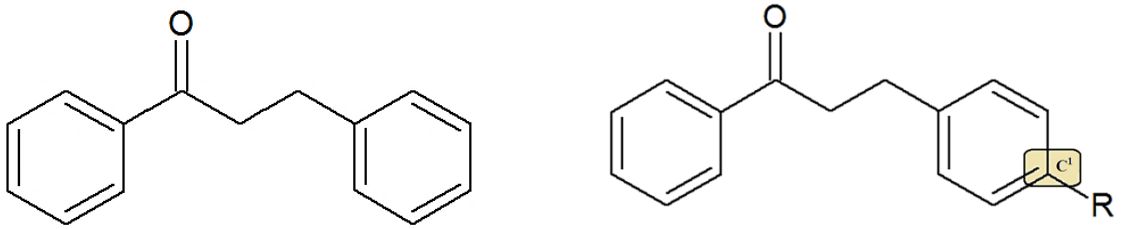

(a) **(b)**

Figure 1. (a) Molecular recognition skeleton (compound 1) used for the molecular alignment and **(b)** Local structural differences (to the substituent effect analysis).

Compound	R	pIC_{50} [b]	CoMSIA [c]	
			Pred.	Δ (error)
1	H [a]	4,80	4,88	0,08
2	chloro	4,84	4,78	-0,06
3	nitro	4,65	4,35	-0,30
4	phenyl	4,58	4,64	0,06
5	fluoro	5,02	4,78	-0,24
6	methoxy	4,60	4,88	0,28
7	quinolinyl	5,70	5,70	0,00
8	ethyl	4,78	4,86	0,08
9	methyl	4,59	4,90	0,31
10	trifluoromethyl	5,52	5,29	-0,23
11	dimethylamino	4,74	4,70	-0,04

[a] Reference compound

[b] Experimental values reported by Liu and co-workers **[15]**.

[c] Theoretical predictions from the CoMSIA method **[12]**.

The CoMSIA method on the molecular set studied is calculated at the intersections of a regularly spaced lattice (1.1 and 2 Å spacing), the similarity indices $A_{F,k}$ between the compounds of interest and a probe atom have been calculated according to:

$$A^{q}_{F,k}(j) = \sum_{i} w_{probe,k} w_{ik} e^{-\alpha r^{2}_{kq}} \qquad \textbf{(1)}$$

Where A is the similarity index at grid point q, summed over all atoms i of the molecule j under investigation; $w_{probe,k}$ probe atom with charge +1, radius 1 Å, hydrophobicity +1, H-bond donor and acceptor property +1; α: attenuation factor; r_{iq}: mutual distance between probe atom at grid point q and atom i of the test molecule **[13]**.

Analysing the equation 1 is possible see the Gaussian function behavior, large values of α will result in a strong attenuation of the distance-dependent consideration of molecular similarity (low global similarity in its neighborhood). The opposite effects (reducing α) means that also the remote parts of each molecule will be experienced by the probe atom (high global similarity in its neighborhood).

3. Theory and Computational Details.

3.1 Molecular Quantum Similarity Indexes.

With the main aim fixed in study the CoMSIA results from the DFT framework, we used the Molecular Quantum Similarity Measures (MQSM). A general definition of MQSM has been made in various papers **[16-19]** the quantum similarity measure Z_{AB} between compounds A and B, with electron density $\rho_A(r_1)$ and $\rho_B(r_2)$ respectively, can be studied on the idea of the minimizing of the expression for the Euclidean distance as:

$$D_{AB} = \left(\int \left| \rho_A(r) - \rho_B(r) \right|^2 dr \right)^{1/2} = \left(\int (\rho_A(r_1))^2 dr_1 + \int (\rho_B(r_2))^2 dr_2 - 2 \int \rho_A(r_1) \rho_B(r_2) dr_1 dr_2 \right)^{1/2} = \sqrt{Z_{AA} + Z_{BB} - 2Z_{AB}} \quad \textbf{(2)}$$

Where Z_{AB} is the overlap integral between the electron density of the compound A and B, Z_{AA} and Z_{BB} are the self-similarity of compounds A and B **[20]**.

In this researcher we have used the Carbó index due to that is very used in the quantum similarity context **[16-20]**:

$$I_{AB} = \frac{\int \int \rho_A(r_1) \rho_B(r_2) dr_1 dr_2}{\sqrt{\left(\int \rho_A(r_1) dr_1 \right)^2 \left(\int (\rho_B(r_2))^2 dr_2 \right)^2}} \quad \textbf{(3)}$$

The main structural difference on the compounds studied (see **Figure 1**) is the carbon atom (C^1), therefore the similarity features can be associated from the local point of view, in this order of ideas is used the Hirshfeld approach to study the local quantum similarity

One of the more useful methods to partitioning of electron density in DFT is the Hirshfeld approach **[21]**. This approach is based on partitioning of electron density $\rho(r)$ in contributions $\rho_{C^1}(r)$. These contributions allow define a concept of atom in a reference system and study its (dis)similarity on a molecular set (i.e.; substituent effect analysis). On the other hand, these contributions are proportional to the weight $w_C(r)$ of the electron density of the isolated compound in the so-called *promolecular density* **[22,23]**. The promolecular density is defined as:

$$\rho_{C^1}^{Prom}(r) = \sum_x \rho_x^0(r) \quad \textbf{(4)}$$

To calculate the contribution of carbon atom (C) in the electron density in a molecule A $\rho_A(r)$ is according to:

$$\rho_{C^1}(r) = w_{C^1}(r) \rho_A(r) \quad \textbf{(5)}$$

In this form, the weight ($w_C(r)$) is obtained as:

$$w_{C^1}(r) = \frac{\rho_{C^1}^0}{\sum_x \rho_x^0(r)} \quad \textbf{(6)}$$

Here $\rho_{C^1}^0(r)$ is the electron density of the isolated carbon atom C^1, (i.e.; the reference electron density) **[24]**. In this sense, the contribution atomic of other carbon atom (C^2) in a molecule B is obtained as:

$$\rho_{C^2,B}(r) = w_{C^2}(r) \rho_B(r) \quad \textbf{(7)}$$

with

$$w_{C^2,B} = \frac{\rho_{C^2,B}^0(r)}{\sum_x \rho_x^0(r)} \quad \textbf{(8)}$$

So we can write the contribution of the asymmetric carbon atom products $\rho_A(r)\rho_B(r)$ as:

$$\rho_{C,AB}(r) = w_{C,AB}(r) \rho_A(r) \rho_B(r) \quad \textbf{(9)}$$

Using the equations (4-9) we can express the numerator Z_{AB} in the Carbó index (equation 3) as:

$$Z_{A,B}^{Local,C} = \frac{Z_{AB}}{\sqrt{Z_{AA}Z_{BB}}} = \frac{\iint w_{C,AB}\rho_A(r)\rho_B(r)dr_A dr_B}{\sqrt{\left(\int w_{C,A}(r)\rho_A(r)dr_A\right)^2\left(\int w_{C,B}(r)\rho_B(r)dr_B\right)^2}} \quad \textbf{(10)}$$

where we can write the global index (equation 3) as local contributions. In this context, using these equations we hope study the local similarity and the substituent effects on the reference carbon atom C^1 (see **Figure 1**).

3.2 Reactivity descriptors in the DFT framework.

Due to the fundamental variable in the MQS field is the electron density naturally there is a relationship between MQS and chemical reactivity, moreover the key feature of quantum similarity lies in the use of the electron density of a molecule. From the DFT point of view physical-chemistry properties such as electrostatic, hydrophobic and hydrogen-bond donor or acceptor properties can be related with global chemical descriptors as chemical potential, hardness, electrophilicity index and local reactivity descriptors as the Fukui Functions.

The chemical potential (μ) can be understood as the tendency that have the electrons to exit of the electron cloud and is calculate according to the equation:

$$\mu \approx \frac{\varepsilon_H + \varepsilon_L}{2} \quad \textbf{(11)}$$

Where (ε_H) is the energy of the (HOMO) and (ε_L) is the energy of the (LUMO) **[25, 26]**. The chemical hardness is defined using the equation (11) according to Pearson et. al. **[27]** and is understood as the opposition to distort the electron cloud of the system according to the equation:

$$\eta \approx \varepsilon_L - \varepsilon_H \quad \textbf{(12)}$$

Using the equation (12), we obtain the softness **[28]** as:

$$S = \frac{1}{\eta} \quad \textbf{(13)}$$

Finally, using the equations 11 and 12 is obtaining the electrophilicity index (ω) **[29, 30]**. This index is understood as the measure of the stabilization energy of the system when it is saturated by electrons from the external environment and is calculated as follows:

$$\omega = \frac{\mu^2}{2\eta} \quad \textbf{(14)}$$

The quantities defined in equations (11-14) are called global reactivity indexes and provide information about the reactivity or stability of a chemical system front to external perturbations. To study the chemical reactivity from the local point of view are used the Fukui Functions. The Fukui Functions (equation 15 and 16, $f(r)$) are defined as the derivative of the electronic density with respect to the number of electrons at constant external potential:

$$f_k^+ \approx \int_k \left[\rho_{N+1}(\vec{r}) - \rho_N(\vec{r})\right] = \left[q_k(N+1) - q_k(N)\right] \quad \textbf{(15)}$$

$$f_k^- \approx \int_k \left[\rho_N(\vec{r}) - \rho_{N-1}(\vec{r})\right] = \left[q_k(N) - q_k(N-1)\right] \quad \textbf{(16)}$$

Where q_k refers to the electron population at k^{th} atomic site in a molecule. Here, we adopted natural population analysis (NPA) scheme to evaluate atomic charge. (f_k^+) governing the susceptibility for nucleophilic attack and (f_k^-) governing the susceptibility for electrophilic attack **[31-33]**.

In this sense, using these global and local reactivity schemes is possible study the selectivity and substituent effect on the molecular set from DFT framework.

3.3 Alignment Method and Computational details.

Similar to the CoMSIA method the MQS also need an optimal alignment methodology, to deal with the problem of the relative molecular alignment is used the Topo-Geometrical Superposition Algorithm (TGSA) **[34]**. This alignment method tries to overlap as many structural elements as possible. These structural elements correspond to chemical bonds and sequences of two chemical bonds, always involving the same type of atoms in both molecules compared **[35-37]**. All the compounds were optimized using B3LYP exchange-correlation functional **[38(a,b)]** at 6-31G(d,p) level of theory. All the optimizations were carried out using Gaussian 09 **[39]**.

Using the Dirac delta distribution $\Omega(r_1, r_2) = \delta(r_1, r_2)$ **[40]** is possible define the so called overlap molecular quantum similarity measure and relates the volume associated with the overlap of the two densities $\rho_A(r)$ and $\rho_B(r)$ according to the equation:

$$Z_{AB}(\Omega) = \iint \rho_A(r_1)\delta(r_1 - r_2)\rho_B(r_2)dr_1dr_2 = \int \rho_A(r)\rho_B(r)dr \quad \textbf{(17)}$$

Equation 17 provides the information about the electron concentration in the molecule and indicates the degree of overlap between the compared compounds.

When the $\Omega(r_1, r_2)$ operator is the coulomb operator $\Omega(r_1, r_2) = |r_1 - r_2|^{-1}$ it represents the electronic coulomb repulsion energy between molecular densities $\rho_A(r)$ and $\rho_B(r)$ as:

$$Z_{AB}(\Omega) = \iint \rho_A(r_1)\frac{1}{|r_1 - r_2|}\rho_B(r_2)dr_1dr_2 \quad \textbf{(18)}$$

Using these operators (equations 17 and 18) we calculate the local quantum similarity through the equation 10. In this sense, the Carbó index is restricted to the range (0,1) where C_{AB}=0 means dis(similarity) and C_{AB}=1 self-similarity, according to the Schwartz integral.

$$\left[\int \rho_A(r)\rho_B(r)dr\right]^2 \leq \int \rho_A^2(r)dr \int \rho_B^2(r)dr \quad \textbf{(19)}$$

Using these methodologies we hope study the substituent effects in the molecular set and shows news insight on the selectivity and chemical reactivity of these antimalarial chalcones.

4. Results and Discussion

The CoMSIA method is a very reliable method for study the structure-activity trend

within biological sets. It is a statistic approach that seeks to correlate relative differences in molecular descriptor values to a dependent property (e.g.; the binding affinity). However, the complexity and complications to understand this 3D QSAR results are increasing. One of the forms to deal these problems can be using the Quantum Similarity field and reactivity descriptors supported on DFT.

In this context, in **Table 2** are shows the local molecular quantum similarity indexes using the operator of overlap (17) and the equation 10. These measures can be related with the steric effects along the molecular set.

The highest values in the local similarity of overlap is between compounds 2 and 9 (0,991) with an euclidean distance of (0,450, see **Table 3**) while the lowest value is between the compounds **7** and **10** (0,682) with an euclidean distance of 3,523. The diagonal corresponds to the self-similarity according to the range of the Carbó index, the main difference between the Carbó indexes and the euclidean distances is that these last can take values from zero to infinity (0,∞). To understand these trends in the molecular set with respect to the reference compound 1 are used the scales of convergence quantitative alpha (α) to steric effects using the **Tables 2** and **3**, respectively (see **Figure 2**).

Despite the steric effect by the chloro atom (compound **2**) with respect to the hydrogen atom (compound **1**), in this **Figure 2** the highest similarity is between these compounds (0,976) with an euclidean distance (3,108), the substituent with most steric effect is trifluoromethyl (compound **10**), and this substituent decreases the quantum similarity in 0,735. Finally, in both trends we can see the same behavior. To analyses the electrostatic effects along the molecular set is shows the **Tables 4** and **5** using the equations 10 and 18.

As **Table 2**, in **Table 4** the highest values in the coulomb similarity is between the compounds **2** and **9** (0,999) with an euclidean distance (0,791, see **Table 5)**, the lowest value is between the compounds **5** and **7** (0,913) with an euclidean distance (20,221), these values shows as the resonance effects cause (dis)similarity along the molecular set. In general, comparing the overlap and coulomb indexes we can see highest values in these last. Therefore, the electrostatic effects can be more relevant than the steric to explain the antimalarial activity.

To study the trends on the molecular set using the coulomb operator with respect to the reference compound **1** is shows in **Figure 3** the scales of convergence quantitative (β) to study the electrostatic effects. The most active compound **7** (see **Table 1**) has the highest values of euclidean distance (22,474) with the compound **1**, this values is agrees with the size of the quinolinyl group and it resonance effect. These good similarity values (**Tables 2-5**) can be related with the cross-validated correlation coefficient (q^2 = 0.704) of the CoMSIA results reported by Xue **[12]** in this context the hybrid methodology (MQS and Chemical reactivity) reported can be independent of the number of molecules used.

In **Figure 3** the highest value is between the compounds **1** and **2** (0,994) with an euclidean distance (22,474) this result is agree with **Figure 2** while the lowest value is between the compounds **1** and **7** (0,893) and an euclidean distance of (4,191). To understand as the MQSM can be considered as QSAR descriptors we used the equation reported by Carbó and co-workers **[41]**. In this equation any physical-chemical property (e.g.; entropy) or biological activity of a molecule (π_I) can be considered to be the

expectation value of an unknown quantum-mechanical observable

$$\pi_I = \langle \Omega(x) \rangle_I = \int \Omega(x) \rho_I(x) dx = \langle \Omega | \rho_I \rangle \quad \textbf{(20)}$$

Being (ρ_I) the density function of molecules I, (**Ω**) represent some quantum-mechanical operator. Using the mean of MQSM is possible obtain the molecular density function projected into a n-dimensional point-molecule vector $\mathbf{Z_I}$, in this context we can approximate the operator (**Ω**) through a vector **w**.

$$\pi_I = \langle \Omega \rangle_I \approx \mathbf{w}^{\mathbf{T}} \mathbf{z_I} \quad \textbf{(21)}$$

In this equation the point operator **w** is unknown a priori; yet its elements can be evaluate using the least-squares fitting for a molecular training set. This equation (21) shows a possible relationship between MQSM and the QSAR field **[42]**.

Due to that the coulomb operator has more incidence in the molecular set (the highest values in the Carbó index see **Tables 2** and **4**) we used the chemical reactivity descriptors. In **Table 6** are shows the global reactivity descriptors such as chemical potential (μ), hardness (η), softness (S) and electrophilicity (ω).

In **Table 5** the reference compound **1** has a chemical potential (μ=-3,9550 eV), hardness (η=4,894 eV), softness (S=0,204 eV^{-1}) and electrophilicity (ω=1,598 eV). However, the compound **7** (quinolinyl as substituent) has the highest chemical potential (μ=-3,622 eV), while that the compound **10** (trifluoromethyl as substituent) has the highest hardness (η=5,133 eV) with softness (S=0,195 eV^{-1}), finally the compound 3 (nitro as substituent) has the highest electrophilicity with (ω=2,353 eV).

Although the compound **3** has the lowest biological activity (pIC_{50}=4,65), this compound has the highest electrophilicity value (ω=2,353 eV). On the other hand, the most active compound **7** (pIC_{50}=5,70) has the highest chemical potential (μ=-3,622 eV) and lowest electrophilicity (ω=1,5351 eV) these results can be related with the no-covalent interactions associated to these antimalarial compounds **[12, 43]**. With these descriptors we can see as the acceptor and donor groups can have influence on the reactivity parameters along the molecular set. To analyses the local reactivity, in **Figure 4** is shows the Fukui Functions on the carbon atom C^1 (see **Figure 1**).

In **Figure 4** are highlight the Fukui Functions $f^{+/-}(r)$ regions, these regions shows the type of stabilization of these compounds on the active site. In this sense, the substituents analyzed increase the chemical activity and the retrodonor process. Additionally, this retrodonor process can determine the stabilization in the active site and the antimalarial activity presented. On the other hand, these Fukui regions are agrees with the docking studies reported by Oliveira and co-workers **[44]** and other works about structure-activity relationship **[45-46]**.

One of the important goals into the QSAR studies is the quantitative correlation of molecular structure with the binding constant and subsequently the prediction of this property for novel compounds. In this sense, this methodology can help to characterize those spatial features that are responsible for activity changes in a series of drug molecules when the receptor is known or not.

Additionally, the entopic changes associated to the molecular set can be understood in term of quantum similarity. Furthermore, the target property to be correlated and predicted in a

comparative analysis is a free energy value. It can be imagined that enthalpic contributions to the binding constant are covered by molecular descriptors that explore the capabilities of molecules to perform intermolecular interactions with a putative receptor, these insights also can be understand in terms of chemical reactivity.

Table 2. Local molecular quantum similarity matrix using the overlap operator (equation 18).

C[a],Ove.[b]	1	2	3	4	5	6	7	8	9	10	11
1	1,000										
2	0,976	1,000									
3	0,849	0,903	1,000								
4	0,866	0,899	0,840	1,000							
5	0,919	0,935	0,867	0,847	1,000						
6	0,902	0,923	0,902	0,886	0,873	1,000					
7	0,798	0,823	0,763	0,791	0,774	0,769	1,000				
8	0,940	0,964	0,881	0,880	0,911	0,901	0,811	1,000			
9	0,964	0,991	0,909	0,897	0,939	0,947	0,819	0,958	1,000		
10	0,735	0,784	0,820	0,753	0,711	0,881	0,682	0,756	0,830	1,000	
11	0,884	0,917	0,893	0,841	0,858	0,867	0,824	0,892	0,921	0,810	1,000

[a] C: compound.

[b] Ove: Overlap Index.

Table 3. Local molecular quantum similarity matrix (MQSM) using the euclidean distance of overlap.

C[a], DO[b]	1	2	3	4	5	6	7	8	9	10	11
1	0,000										
2	0,757	0,000									
3	2,115	1,731	0,000								
4	1,926	1,685	2,229	0,000							
5	1,497	1,337	2,019	2,113	0,000						
6	1,604	1,429	1,727	1,808	1,886	0,000					
7	2,531	2,382	2,830	2,621	2,708	2,728	0,000				
8	1,219	0,943	1,894	1,831	1,565	1,625	2,458	0,000			
9	0,916	0,450	1,672	1,698	1,299	1,201	2,408	1,021	0,000		
10	3,108	2,850	2,639	3,041	3,269	2,190	3,523	3,004	2,586	0,000	
11	1,765	1,509	1,814	2,151	2,014	1,937	2,398	1,719	1,473	2,688	0,000

[a] C: compound.

[b] DO: Euclidean Distance of Overlap.

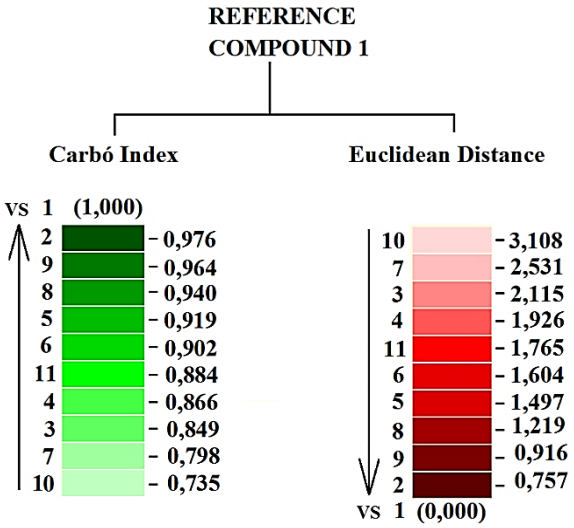

Figure 2. Scales of convergence quantitative α to steric effects proposed to the reference compound 1.

Table 4. Local molecular quantum similarity matrix using the coulomb operator (equation 19).

C[a],Cou.[b]	1	2	3	4	5	6	7	8	9	10	11
1	1,000										
2	0,994	1,000									
3	0,964	0,986	1,000								
4	0,939	0,962	0,975	1,000							
5	0,990	0,997	0,983	0,955	1,000						
6	0,978	0,991	0,991	0,973	0,988	1,000					
7	0,893	0,920	0,939	0,961	0,913	0,932	1,000				
8	0,982	0,993	0,987	0,971	0,989	0,991	0,932	1,000			
9	0,993	0,999	0,986	0,962	0,997	0,991	0,920	0,993	1,000		
10	0,936	0,965	0,986	0,971	0,959	0,981	0,944	0,973	0,967	1,000	
11	0,965	0,984	0,992	0,975	0,979	0,984	0,952	0,984	0,984	0,984	1,000

[a] C: compound.

[b] Cou: Coulomb Index.

Table 5. Local molecular quantum similarity matrix (MQSM) using the Euclidean Distance of coulomb.

C[a], DC[b]	1	2	3	4	5	6	7	8	9	10	11
1	**0,000**										
2	**4,191**	**0,000**									
3	**10,896**	**7,135**	**0,000**								
4	**15,129**	**12,11**	**9,325**	**0,000**							
5	**5,331**	**2,920**	**7,472**	**12,741**	**0,000**						
6	**8,178**	**5,096**	**5,228**	**9,946**	**5,973**	**0,000**					
7	**22,474**	**19,799**	**16,786**	**13,299**	**20,221**	**17,989**	**0,000**				
8	**7,431**	**4,433**	**6,315**	**10,422**	**5,361**	**4,821**	**18,046**	**0,000**			
9	**4,318**	**0,791**	**7,120**	**12,172**	**2,857**	**4,939**	**19,831**	**4,443**	**0,000**		
10	**15,507**	**11,891**	**7,284**	**9,841**	**12,422**	**8,779**	**15,519**	**10,271**	**11,671**	**0,000**	
11	**10,851**	**7,474**	**4,863**	**9,190**	**8,171**	**6,902**	**15,268**	**6,817**	**7,435**	**7,472**	**0,000**

[a] C: compound.

[b] DC: Euclidean Distance of Coulomb.

5. Conclusions

This work shows how the CoMSIA results can be understood in terms of (MQS) and Chemical reactivity descriptors. To carry out this aim, were used the CoMSIA results reported by Xue and coworkers **[12]**, this CoMSIA study is carried out on a serie of antimalarials chalcones.

The hybrid methodology reported, shows the steric and electrostatic effects in form of the scales of convergence quantitative convergence alpha (α) to steric effects and beta (β) to electrostatic effects, these scales allow study the substituent effects and were constructed using the reference compound 1 (hydrogen as substituent on the reference carbon C^1). These results were completed with a reactivity study using global and local descriptors such as chemical hardness, softness, electrophilicity, and Fukui Functions.

In this sense, the CoMSIA results reported by Xue **[12]** were modeled joining MQS and chemical reactivity; in this context these outcomes can be applied in QSAR correlations and docking studies to understand the antimalarial activity of these compounds. Taking into account that this methodologies can be used when the receptor is known or even when it is not known.

Acknowledgments

A.M.B thanks to the Universidad de Talca (CBSM)) for the continuous support to this investigation and to the postdoctoral project N^0 3150035 (FONDECYT, CHILE).

Conflicts of Interest

The authors declare no conflict of interest.

References and Notes

1. Morales-Bayuelo A, Matute R A, Caballero J 2015 J. Mol. Model. 21, 156.
2. Carbó-Dorca R, Arnau M, Leyda L 1980 Int. J. Quant. Chem. 17, 1185.
3. Amat L, Carbó-Dorca R 2002 Int. J. Quant. Chem. 87, 59.
4. Gironés X, Carbó-Dorca R 2006 QSAR Comb. Sci. 25, 579.
5. Carbó-Dorca R, Gironés X 2005 Int. J. Quat. Chem. 101,8.
6. Bultinck P, Rafat M, Ponec R, Gheluwe B V, Carbó-Dorca R, Popelier P 2006 J. Phys. Chem. A. 110, 7642.
7. Robert D, Amat L, Carbó-Dorca R 1999 J. Chem. Inf. Comp. Sci. 39, 333.
8. (a) Morales-Bayuelo A, Vivas-Reyes R. 2013 J. Math. Chem. 51, 125. (b) Morales-Bayuelo A, Vivas-Reyes R. 2013 J. Math. Chem. 51, 1835. (c) Morales-Bayuelo A, Torres J, Vivas-Reyes R 2012 J. Theor. Comput. Chem. 11, 1. (d) Morales-Bayuelo A, Vivas-Reyes R. 2014 J. Quant. Chem. Article ID 239845, 19 pages. (e) Morales-Bayuelo A, Vivas-Reyes R. J. Quant. Chem. 2014, Article ID 850163, 12 pages.
9. Parr R G, Yang W 1989 Density Functional Theory of Atoms and Compounds; Oxford University Press: New York.
10. Geerlings P, De Proft F, Langenaeker W, 2003 Chem. Rev. 103, 1793.
11. Parr RG, Chattaraj PK. 1991 J. Am. Chem. Soc. 113, 1854.
12. Xue CX, Cui SY, Liu MC, Hu ZD, Fan BT 2004 Eur. J. Med. Chem. 39, 745.
13. Klebe G, Abraham U 1999 J. Comp.-Aided Mol. Design. 13, 1.
14. Klebe G, Abraham U, Mietzner T 1994 J. Med. Chem. 37, 4130.
15. Liu M, Wilairat P, Go PM 2001 J. Med. Chem. 44, 4443.
16. Carbó-Dorca R, Arnau M, Leyda L 1980 Int. J. Quant. Chem. 17, 1185.
17. Amat L, Carbó-Dorca R 2002 Int. J. Quant. Chem. 87, 59.
18. Gironés X, Carbó-Dorca R 2006 QSAR Comb. Sci. 25, 579.
19. Carbó-Dorca R, Gironés X 2005 Int. J. Quant. Chem. 101,8.
20. Bultinck P, Gironés X, Carbó-Dorca R (2005) Rev. Comput. Chem. 21,127.
21. Hirshfeld F L 1977 Theor. Chim. Acta. 44, 129.
22. De Proft F, Van Alsenoy C, Peeters A, Langenaeker W, Geerlings P 2002 J. Comput. Chem. 23, 1198.
23. Randic M, Johnson M A, Maggiora G M 1990. In Concepts and Applications of Molecular Similarity, Design of Compounds with Desired Properties. Eds., Wiley-Interscience. New York. 77.
24. (a) Boon G, Van Alsenoy C, De Proft F, Bultinck P, Geerlings P 2005 J. Mol. Struct. 727, 49. (b) Morales-Bayuelo A, Caballero, J. 2015 J. Mol. Mod. 21, 45.
25. Ayers P W, Anderson J S M, Bartolotti L J 2005 Int. J Quant. Chem. 101, 520.
26. Harbola MK, Chattaraj PK, Parr RG 1991 Isr. J. Chem. 31, 395.
27. Pearson R G 1997 Chemical Hardness; Applications from Compounds to Solids; Wiley-VHC, Verlag GMBH: Weinheim, Germany.
28. Yang W T, Parr R G 1985 Proc. Natl. Acad. Sci. 82, 6723.
29. Chattaraj PK, Sarkar U, Roy DR 2006 Chem. rev. 106, 2065.
30. Ayers P, Parr R G 2000 J. Am. Chem. Soc. 122, 2010.

31. Galván M, Pérez P, Contreras R, Fuentealba P 1999 Chem. Phys. Lett. 30, 405.
32. Mortier W J, Yang W 1986 J. Am. Chem. Soc. 108, 5708.
33. Fuentealba P, Pérez P, Contreras R 2000 J. Chem. Phys. 113, 2544.
34. Girones X, Robert D, Carbó-Dorca R 2001 J. Comput. Chem. 22, 255.
35. Carbó-Dorca R, Besalú E, Amat L, Fradera X 1995 J. Math. Chem. 18, 237.
36. Besalú E, Girones X, Amat L, Carbó-Dorca R 2002 Acc. Chem. Res. 35, 289.
37. Boon G, Langenaeker W, De Proft F, De Winter H, Tollenaere JP, Geerlings 2001 P J. Phys. Chem. A. 105, 8805.
38. (a) Becke A. D 1988 Phys. Rev. A. 38, 3098, (b) Lee C, Yang W, Parr R G 1988 Phys. Rev. B. 37, 785.
39. GAUSSIAN 09, Revision C.01, Frisch M J, G. Trucks W, Schlegel H B, Scuseria G E, Robb M A, Cheeseman J R, Scalmani G, Barone V, Mennucci B, Petersson G A, Nakatsuji H, Caricato M, Li X, Hratchian H P, Izmaylov A F, Bloino J, Zheng G, Sonnenberg J L, Hada M, Ehara M, Toyota K, Fukuda R, Hasegawa J, Ishida M, Nakajima T, Honda Y, Kitao O, Nakai H, Vreven T, Montgomery J A Jr., Peralta J E, Ogliaro F, Bearpark M, Heyd J J, Brothers E, Kudin K N, Staroverov V N, Keith T, Kobayashi R, Normand J, Raghavachari K, Rendell A, Burant J C, Iyengar S S, Tomasi J, Cossi M, Rega N, Millam J M, Klene M, Knox J E, Cross J B, Bakken V, Adamo C, Jaramillo J, Gomperts R, Stratmann R E, Yazyev O, Austin A J, Cammi R, Pomelli C, Ochterski J W, Martin R L, Morokuma, K. Zakrzewski V G, Voth G A, Salvador P, Dannenberg J J, Dapprich S, Daniels A D, Farkas O, Foresman J B, Ortiz J V, Cioslowski J, and Fox D J, Gaussian, Inc., Wallingford CT. 2010.
40. Arfken GB, Weber HJ (2000) Mathematical methods for physicists, 5th edn. Academic, Boston.
41. Carbó-Dorca R, Besalu E, Amat L, Fradera X 1996 J. Math. Chem. 19, 47.
42. Fradera X, Amat L, Besalú E, Carbó-Dorca R 1997 Quant. Struct.-Act. Relat. 16, 25.
43. Oliveira M, Cenzi G, Nunes RR, Andrighetti, Valadão D MS, Reis C, Oliveira Simões CM, Nunes RJ, Júnior MC, Taranto AG, Sanchez BAM, Viana GHR Varotti FP 2013 Molecules. 18, 15276.
44. Rongshi L, Kenyon G, Cohen FE, Chen X, Gong B, Dominguez JN, Davidson E, Kurzban G, Miller RE, Nuzum EO, Rosenthal PJ, McKerrow JH 1995 J. Med. Chem. 38, 5031.
45. Domínguez JN, León C, Rodrigues J, Domínguez DG, Gut J, Rosenthal PJ. 2005 Farmaco I. 60, 307.
46. Tomar V, Bhattacharjee G, Kamaluddin S, Rajakumar KS, Puri SK 2010 Eur. J. Med. Chem. 45, 2745.